

Reflection Symmetric Ballistic Microstructures: Quantum Transport Properties

Harold U. Baranger¹ and Pier A. Mello²

¹ Bell Laboratories— Lucent Technologies, 700 Mountain Ave. 1D-230, Murray Hill NJ 07974

² Instituto de Física, Universidad Nacional Autónoma de México, 01000 México D.F., Mexico

(Submitted to Phys. Rev. Lett. 22 July 1996)

We show that reflection symmetry has a strong influence on quantum transport properties. Using a random S -matrix theory approach, we derive the weak-localization correction, the magnitude of the conductance fluctuations, and the distribution of the conductance for three classes of reflection symmetry relevant for experimental ballistic microstructures. The S -matrix ensembles used fall within the general classification scheme introduced by Dyson, but because the conductance couples blocks of the S -matrix of different parity, the resulting conductance properties are highly non-trivial.

PACS numbers: 72.20.My, 05.45.+b, 72.15.Gd

The effect of symmetry on the quantum corrections to the conductance is one of the main themes of mesoscopic physics. Perhaps most familiar is the suppression of the average quantum conductance at zero magnetic field because of time-reversal symmetry, an effect known as weak-localization. Previous work has concentrated on the effects of time-reversal and spin-rotational invariance on transport through disordered conductors [1].

The advent of clean microstructures, in which transport is largely ballistic [1,2,3], opens the possibility of studying different spatial reflection symmetries. In these structures the electrons move in a potential largely determined by lithography, and structures of definite reflection symmetry, as well as of adjustable symmetry, are possible. Alternatively, reflection symmetric scattering systems could be probed in microwave cavities [4]. Our goal here is to determine how such reflection symmetries affect the interference contribution to transport.

Because conductance is related to scattering from the system, the symmetry classes for quantum transport are closely related to those for the scattering matrix S . It has been shown [5,6,7,8] that ensembles in which S is distributed with an “equal-a-priori probability” across the available matrix space provide a good description of the statistical properties of quantum transport when (1) the classical dynamics is chaotic, (2) direct processes through the system are ruled out, and (3) there are no spatial symmetries. The symmetry classes for such S -matrices were introduced by Dyson [9,10].

In Dyson’s scheme there are three basic symmetry classes. In the absence of any symmetries, the only restriction on S is unitarity due to flux conservation: this is the *unitary* case, denoted $\beta=2$. In the *orthogonal* case ($\beta=1$), S is symmetric because one has either time-reversal symmetry and integral spin or time-reversal symmetry, half-integral spin and rotational symmetry. In the *symplectic* case ($\beta=4$), S is self-dual because of time-reversal symmetry with half-integral spin and no rotational symmetry. The intuitive idea of “equal a priori

probability” is expressed mathematically by the measure on the matrix space which is invariant under the symmetry operations for the class in question. This notion of *invariant measure* gives rise to the *circular* orthogonal, unitary and symplectic *ensembles* (*COE*, *CUE*, *CSE*).

In the presence of additional symmetries, for fixed values for all quantum numbers of the full symmetry group, the invariant ensemble is one of the three circular ensembles [9]. Thus for reflection symmetries, S is block diagonal in a basis of definite parity with respect to reflection, with a circular ensemble in each block. This is the natural representation for the eigenvalues of S , and the statistics of eigenvalues for such independent superpositions have been studied previously [9,10]. However, the conductance of a system is *not* an eigenvalue property: it depends on the properties of the scattering *wave-functions*, and those appropriate for the conductance are not necessarily of definite reflection parity. Hence the conductance may couple the different parity-diagonal blocks of S , and the resulting quantum transport properties are a non-trivial generalization of the circular ensemble results.

In this paper we investigate the effects of three classes of reflection symmetry on the quantum scattering properties of classically chaotic systems [11]. We consider two-dimensional systems with spinless particles and rule out any direct processes. The three classes are (1) *Up-down* (*UD*)— reflection through an axis parallel to the current, (2) *Left-right* (*LR*)— reflection through an axis perpendicular to the current, and (3) *Four-fold* (*4F*)— the combination of up-down and left-right. The resulting statistical distribution of the transmission T through the system is calculated. The predictions compare favorably with numerical calculations in which the Schrödinger equation is solved for a number of structures.

Structure of the S-matrix— Consider (spinless) single-electron scattering by a ballistic quantum dot connected to the outside by two leads, each supporting N propagating modes. The $2N$ -dimensional S matrix, which relates the incoming amplitudes from the left and right $\{a^{L,R}\}$

TABLE I. The structure of the S matrix for up-down (UD), left-right (LR), and four-fold (4F) reflection symmetry.

	$B = 0$	$B \neq 0$
UD	$\begin{bmatrix} r_e & t_e^T & 0 \\ t_e & r_e & \\ 0 & r_o & t_o^T \\ & t_o & r_o \end{bmatrix}$ $r_{e,o} = r_{e,o}^T, \quad r'_{e,o} = r'_{e,o}^T$	$\begin{bmatrix} r & t^T \\ t & r' \end{bmatrix}$ $r = r^T, \quad r' = r'^T$
LR	$\begin{bmatrix} r & t \\ t & r \end{bmatrix}$ $r = r^T, \quad t = t^T$	$\begin{bmatrix} r & t' \\ t & r^T \end{bmatrix}$ $t = t^T, \quad t' = t'^T$
4F	$\begin{bmatrix} r_e & t_e & 0 \\ t_e & r_e & \\ 0 & r_o & t_o \\ & t_o & r_o \end{bmatrix}$ $r_{e,o} = r_{e,o}^T, \quad t_{e,o} = t_{e,o}^T$	$\begin{bmatrix} r & t \\ t & r \end{bmatrix}$ $r = r^T, \quad t = t^T$

to the outgoing ones $\{b^{L,R}\}$, is

$$\begin{bmatrix} b^L \\ b^R \end{bmatrix} = S \begin{bmatrix} a^L \\ a^R \end{bmatrix}; \quad S = \begin{bmatrix} r & t' \\ t & r' \end{bmatrix}, \quad (1)$$

where r, r' are the $N \times N$ reflection matrices for incidence from each lead and t, t' the corresponding transmission matrices. The conductance is given in terms of the transmission coefficient $T = \text{tr}[tt^\dagger]$ by $G = (e^2/h)T$ [1].

The reflection symmetries indicated above impose restrictions on S : the resulting structure, both in the absence and in the presence of a magnetic field B , is presented in Table I, which we now discuss.

First, for $B = 0$, the wave functions in the leads are $\exp(ik_n x)\chi_n(y)$ where the channel wave functions $\chi_n(y)$ vanish at the walls of the leads. For UD symmetry, S contains two disconnected symmetric S matrices, for the even (e) and odd (o) parity channels, respectively. For LR, changing $x \rightarrow -x$ in the wave function gives a solution for the same energy: consistency with Eq. (1) and $S = S^T$ (from time-reversal invariance) gives the structure shown. By transforming to states of definite parity, S in the LR case becomes block diagonal with the matrices $S_\pm \equiv r \pm t$ on the diagonal; hence S is fundamentally a superposition of two symmetric S matrices as for UD. A similar procedure is used to analyze 4F symmetry.

Second, for a uniform B in the z -direction, the Schrödinger equation in the Landau gauge is

$$\left[\frac{1}{2m} \left(p_x - \frac{e}{c} B y \right)^2 + \frac{p_y^2}{2m} + V \right] \psi = E \psi. \quad (2)$$

General consequences of the spatial symmetry of $V(x, y)$ now follow. For UD symmetry, $V(x, y) = V(x, -y)$, so that $\psi^*(x, -y)$ satisfies Eq. (2). We thus have the antiunitary symmetry $R_x \vartheta$, where R_x is the reflection operator

TABLE II. The invariant measure for the S matrix for three reflection symmetry classes. $d\mu^{(1)}$ is the COE measure.

	$B = 0$	$B \neq 0$
UD	$d\mu^{(1)}(S_e) d\mu^{(1)}(S_o)$	$d\mu^{(1)}(S)$
LR	$d\hat{\mu}^{(1)}(S) \equiv d\mu^{(1)}(S_+) d\mu^{(1)}(S_-)$	$d\mu^{(1)}(S)$
4F	$d\hat{\mu}^{(1)}(S_e) d\hat{\mu}^{(1)}(S_o)$	$d\hat{\mu}^{(1)}(S)$

with respect to the x axis and ϑ is the time-reversal operator. For LR, $V(x, y) = V(-x, y)$, $\psi^*(-x, y)$ satisfies Eq. (2), and we have the antiunitary symmetry $R_y \vartheta$, with R_y the reflection operator with respect to the y axis. For 4F, both $R_x \vartheta$ and $R_y \vartheta$ are relevant. We now consider a scattering problem in which the basic wave functions in the leads are $\exp(ik_n x)\chi_{nk}(y)$. For UD symmetry, application of $R_x \vartheta$ leads to $S = S^T$ [12]. For LR, $R_y \vartheta$ gives $(\Sigma_x S) = (\Sigma_x S)^T$, where $\Sigma_x = \begin{bmatrix} 0_N & 1_N \\ 1_N & 0_N \end{bmatrix}$ and 0_N and 1_N are the $N \times N$ zero and unit matrices, respectively. Finally, for 4F one finds $S = S^T$ and $(\Sigma_x S) = (\Sigma_x S)^T$, so that S has the same structure as for LR at $B = 0$. These results lead to the structure of S shown in Table I.

Invariant measure— The invariant measure is most easily written down in a basis of definite parity with respect to all symmetry operators. In this case, it is simply a product of circular ensemble measures $d\mu^{(\beta)}(S)$ for each block of S ; results are presented in Table II. Thus for $B = 0$, the invariant measure for both UD and LR symmetry is a product of two COE. For $B \neq 0$, because of the single antiunitary symmetry present for both UD and LR, the ensemble is a single COE. For LR note that *the roles of r and t are reversed* from the usual case.

Statistical properties of T — Once the invariant measure is known, the statistical properties of the transmission are found by integrating over the measure, for instance $\langle T \rangle = \int T d\mu(S)$. Such averages can be calculated explicitly using known properties of unitary and orthogonal matrices [7,8,13]. In Tables III, IV and V we present results for the weak-localization correction (WLC) $\langle T \rangle - N/2$, the variance of T , and the probability density $w(T)$. We now discuss these results.

For UD symmetry, the independent even and odd channels at $B = 0$ imply that the average and variance of T are simply the sum of the COE results for each parity class while the distribution is the convolution. For $B \neq 0$, one obtains the usual COE results.

For LR symmetry, at $B = 0$ one has both coherent back-scattering and coherent *forward*-scattering ($t = t^T$), so that the WLC is identically zero. When $B \neq 0$, the coherent back-scattering is destroyed but the coherent forward-scattering remains because of the $R_y \vartheta$ symmetry. Thus the average transmission is *larger* than the classical value $N/2$, an unusual result for spinless particles. In the probability density $w(T)$ for $N = 1$, the coherent forward scattering produces a square-root singularity at $T = 1$; thus for $B = 0$, $w(T)$ has singularities

TABLE III. The weak-localization correction $\langle T \rangle - N/2$ for three classes of reflection symmetry. Note that this quantity is *positive* for LR symmetry in a magnetic field while the magnetoconductance is zero for 4F symmetry.

	$B = 0$	$B \neq 0$
UD	$-\sum_{i=e,o} N_i/(4N_i + 2)$	$-N/(4N + 2)$
LR	0	$N/(4N + 2)$
4F	0	0

TABLE IV. $\text{var } T$ for three classes of reflection symmetry. Greater symmetry produces larger fluctuations.

	$B = 0$	$B \neq 0$
UD	$\sum_{i=e,o} \frac{N_i(N_i+1)^2}{(2N_i+1)^2(2N_i+3)}$	$\frac{N(N+1)^2}{(2N+1)^2(2N+3)}$
LR	$N/(4N + 4)$	$\frac{N(N+1)^2}{(2N+1)^2(2N+3)}$
4F	$\sum_{i=e,o} N_i/(4N_i + 4)$	$N/(4N + 4)$

at both $T=0$ and $T=1$. For $N=2$ and $B=0$, note the logarithmic singularity in $w(T)$ at $T=1$.

For 4F symmetry, there is sufficient symmetry so that both coherent back-scattering and coherent forward-scattering exist at $B \neq 0$. Thus the WLC is identically zero at both $B=0$ and $B \neq 0$, and so *the average magnetoconductance is zero*. Finally, notice the large variance in this case: $\text{var } T \rightarrow 1/2$ as $N \rightarrow \infty$ for $B=0$.

Numerical calculations— The above predictions are compared, in Figs. 1 to 3, with calculations in which the Schrödinger equation is solved for several billiards using the methods of Ref. [14]. Typical billiards are sketched in the figures: reflection symmetric structures are generated from an asymmetric structure by simply applying the symmetry operators. Note that stoppers block both the direct transmission and the whispering gallery trajectories [7,15,16]. The theoretical ensemble averages are compared with numerical energy averages using 100 energies for each N spaced further than the correlation length. To improve statistics, an additional average was taken over six similar structures differing in the location

	$B = 0$	$B \neq 0$
UD	$\begin{cases} 1/\sqrt{4T} \\ \pi/4, \\ \frac{1}{2} \sin^{-1} \frac{2-T}{T} \end{cases}$	$\begin{cases} 1/\sqrt{4T} \\ 3T/2 \\ \frac{3}{2}(T - 2\sqrt{T-1}) \end{cases}$
LR	$\frac{1}{\pi} \ln \frac{1 + \sqrt{\pi^2 T(1-T)}}{ 1-T }$	$\begin{cases} 1/\sqrt{4(1-T)} \\ \frac{3}{2}(2-T - 2\sqrt{1-T}) \\ \frac{3}{2}(2-T) \end{cases}$
4F	$\frac{1}{\pi^2} K(\sqrt{\pi^2 T(1-T)})$	$\frac{1}{\pi} \ln \frac{1 + \sqrt{\pi^2 T(1-T)}}{ 1-T }$

TABLE V. Probability distribution $w(T)$ for three classes of reflection symmetry. $N=1$ (2) in the upper (lower) half of each entry. For $N=2$ the braces contain results for $0 < T < 1$ on the upper line and for $1 < T < 2$ on the lower one. (K is the complete elliptic integral.)

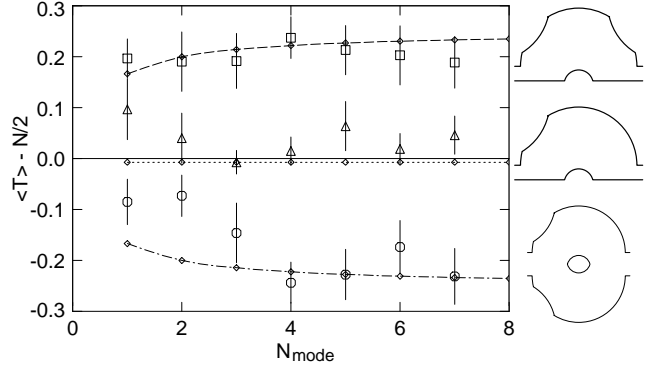


FIG. 1. The weak-localization correction for $B \neq 0$ as a function of the number of modes in the lead: asymmetric (dotted, triangles), up-down (dot-dashed, circles), and left-right (dashed, squares) structures. Lines are theoretical results from Table III (and Ref. [7] for the asymmetric case); symbols with statistical error bars are numerical results averaged over $BA/\phi_0 = 2, 4$. Typical cavities are shown on the side. The presence of symmetry has a strong effect and can produce either a positive or negative correction.

of the stoppers. The classical transmission probability is within 0.005 of 0.5 for all structures.

Fig. 1 shows the weak-localization correction (WLC) as a function of N for $B \neq 0$. The effect of symmetry is striking: the WLC is zero in the absence of symmetry, negative for UD symmetry, and positive for LR. As noted above, $\langle T \rangle$ is larger than the classical transmission ($N/2$) in the LR case (coherent forward-scattering).

Fig. 2 shows the magnetic field dependence of $\text{var } T$. Applying a field causes a crossover between symmetry classes. While the present model does not describe this cross-over, our random matrix theory does predict the limits $B=0$ and $BA/\phi_0 \gtrsim 2$ (as long as $\langle S \rangle \approx 0$ — for much larger fluxes this no longer holds and we enter a different regime [15,16]). Notice that the magnitude of the

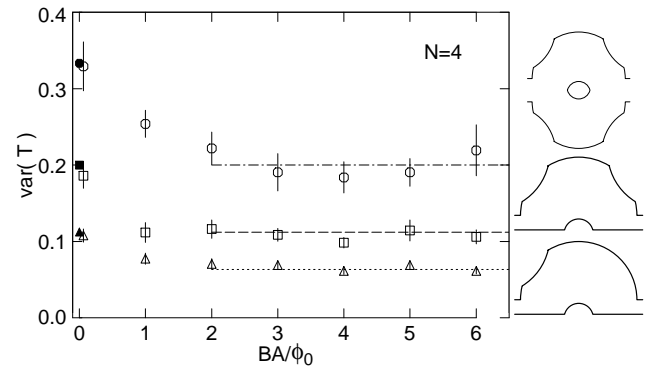


FIG. 2. Variance of the transmission for $N=4$ as a function of magnetic field: asymmetric (dotted, triangles), left-right (dashed, squares), and four-fold (dot-dashed, circles) structures. Lines and solid symbols are theoretical results (Table IV and Ref. [7]); open symbols with statistical error bars are numerical results. The magnitude of the conductance fluctuations increases as the degree of symmetry increases.

conductance fluctuations increases considerably as one moves from asymmetric to LR to 4F structures.

The agreement between theory and numerics is very good in both Figs. 1 and 2. In fact, we find that the agreement for $\text{var } T$ is already good for individual structures. This is good evidence that $\text{var } T$ is a truly universal quantity for spatially symmetric quantum billiards, as long as the classical dynamics is strongly chaotic and direct processes are absent. We cannot say the same for the WLC. While the agreement is good once we average over six structures, we have found a non-negligible sample to sample variation. Thus the WLC is of a less universal character than the variance and may need, for its description, further sample-specific information.

Fig. 3 shows $w(T)$ for the LR case with $N = 1, 2$. These distributions are very different from those for the asymmetric case [7,8]. There are a number of striking features: (a) for $B=0, N=1$, the distribution has maxima at $T=0$ and 1; (b) for $B \neq 0, N=1$, the maximum is at $T=1$; (c) for $N=2$, the data near $T=1$ are consistent with the theoretical logarithmic singularity for $B=0$ and the square-root singularity for $B \neq 0$.

Summary— We have shown, first, that reflection symmetry has a large effect on the quantum transport properties of classically chaotic billiards and, second, that the extended circular ensemble random matrix theory describes these structures well. Because the conductance may couple the different parity-diagonal blocks of S , the quantum transport properties are not a simple superposition of circular ensemble properties. This work indicates that the full statistical distribution of the conductance

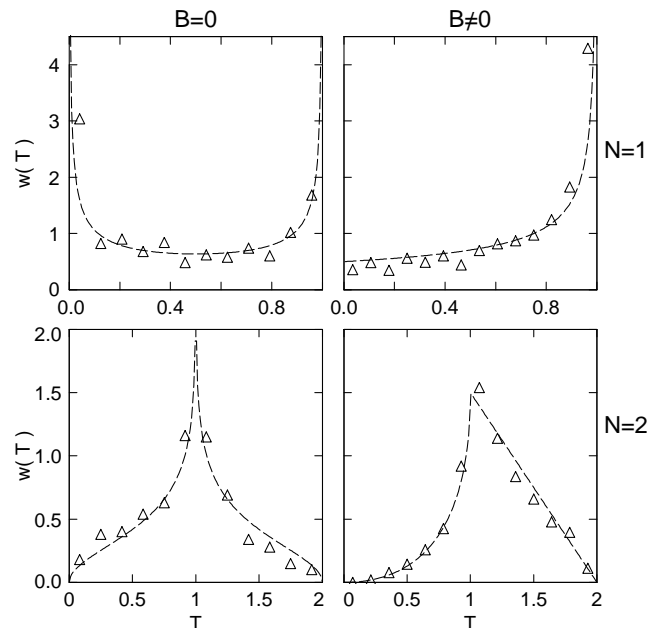


FIG. 3. The probability density of the transmission for left-right symmetry: for $N=1, 2$ and both $B=0$ and $B \neq 0$. The dashed lines are random-matrix theory results from Table V; the triangles are numerical results.

is the same (“universal”), with some reservations for its centroid, for systems that (a) have the same spatial symmetry, (b) show hard chaos classically, and (c) lack direct processes. Experiments observing spatial symmetry effects should be possible in both microwave cavities and mesoscopic systems. The effect of the unavoidable deviations from perfect symmetry can be estimated semiclassically along the lines of Ref. [17], and the results suggest that the best current material [2,3] is sufficiently clean.

- [1] *Mesoscopic Phenomena in Solids*, edited by B.L. Altshuler, P.A. Lee, and R.A. Webb (North-Holland, New York, 1991).
- [2] C.M. Marcus, A.J. Rimberg, R.M. Westervelt, P.F. Hopkins and A.C. Gossard, Phys. Rev. Lett. **69**, 506 (1992); I.H. Chan, *et al.*, Phys. Rev. Lett. **74**, 3876 (1995).
- [3] A.M. Chang, H.U. Baranger, L.N. Pfeiffer, and K.W. West, Phys. Rev. Lett. **73**, 2111 (1994).
- [4] See, e.g., J. Stein, H.-J. Stöckman, and U. Stoffregen, Phys. Rev. Lett. **75**, 53 (1995); A. Kudrolli, V. Kidambi, and S. Sridhar, Phys. Rev. Lett. **75**, 822 (1995).
- [5] R. Blümel and U. Smilansky, Phys. Rev. Lett. **60**, 477 (1988); **64**, 241 (1990); E. Doron and U. Smilansky, Nucl Phys. **A545**, C455 (1992).
- [6] S. Iida, H.A. Weidenmüller, and J.A. Zuk, Ann. Phys. (N.Y.) **200**, 219 (1990); C.H. Lewenkopf and H.A. Weidenmüller, Ann. Phys. (N.Y.) **212**, 53 (1991).
- [7] H.U. Baranger and P.A. Mello, Phys. Rev. Lett. **73**, 142 (1994).
- [8] R.A. Jalabert, J.-L. Pichard, and C.W.J. Beenakker, Europhys. Lett. **27**, 255 (1994).
- [9] F.J. Dyson, J. Math. Phys. **3**, 140 (1962); **3**, 1199 (1962).
- [10] M.L. Mehta, *Random Matrices* (Academic, New York, 1991); C.E. Porter, *Statistical Theories of Spectra: Fluctuations* (Academic, New York, 1965).
- [11] For the unrealistic but instructive case of reflection-symmetric *disordered* conductors see M.B. Hastings, A.D. Stone, and H.U. Baranger, Phys. Rev. B **50**, 8230 (1994).
- [12] M. Robnik and M.V. Berry, J. Phys. A **19**, 669 (1986).
- [13] V.A. Gopar, M. Martínez, P.A. Mello, and H.U. Baranger, J. Phys. A **29**, 881 (1996).
- [14] H.U. Baranger, D.P. DiVincenzo, R.A. Jalabert, and A.D. Stone, Phys. Rev. B **44**, 10 367 (1991).
- [15] H.U. Baranger and P.A. Mello, Europhys. Lett. **33**, 465 (1996)
- [16] Using an average over surface roughness disorder, we find $\langle S \rangle \approx 0$ which justifies our use of the invariant measures. The fact that this is true only in structures with stoppers highlights the importance of blocking short paths.
- [17] K. Richter, D. Ullmo, and R.A. Jalabert, Phys. Rev. B, in press (1996).